Available online at www.sciencedirect.com
ScienceDirect
Solid State Communications 145 (2008) 487–492
solid state communications
www.elsevier.com/locate/ssc

Raman spectroscopic study of LiH_2PO_4

Kwang-Sei Lee[a,*], Jae-Hyeon Ko[b], Joonhee Moon[a], Sookyoung Lee[a], Minhyon Jeon[a]

[a] Department of Nano Systems Engineering, Center for Nano Manufacturing, Inje University, Gimhae 621-749, Gyeongnam, Republic of Korea
[b] Department of Physics, Hallym University, 39 Hallymdaehak-gil, Chuncheon 200-702, Republic of Korea

Received 24 November 2007; accepted 13 December 2007 by D.J. Lockwood
Available online 23 December 2007

Abstract

The dielectric constant of polycrystalline LiH_2PO_4 has been measured between 297 and 17 K. No marked changes were observed over this range, indicating that the room-temperature orthorhombic phase persisted up to 17 K. Raman spectra of polycrystalline LiH_2PO_4 were also measured at 297, 200, and 70 K in the frequency shift region of 15–4000 cm^{-1} with Raman-active vibrational modes naively assigned to low-frequency (0–300 cm^{-1}) external and high-frequency (300–4000 cm^{-1}) internal modes. In addition to the internal modes of the PO_4 tetrahedra, the internal modes of the LiO_4 tetrahedra spectroscopically manifested themselves between 390–500 cm^{-1}. This frequency range overlaps those of ν_2 (PO_4) and ν_4 (PO_4). The LiH_2PO_4O–H vibrational frequencies were in good agreement with crystallographic reports that there are two types of hydrogen bonds: intermediate (long bonds) and strong (short bonds).

PACS: 63.20.Dj; 77.80.-e; 77.84.Fa; 78.30.-j

Keywords: A. Insulators; C. Crystal structure and symmetry; D. Phonons; E. Inelastic light scattering

1. Introduction

MX_2RO_4-type (M = K, Rb, NH_4, Cs, Tl; X = H, D; R = P, As) crystals undergo ferroelectric or antiferroelectric phase transitions at low temperatures [1,2]. They are also known to exhibit high-temperature phase transitions (HTPT), as reported in this class of materials by many investigators. However, the experimental investigations of HTPT, *e.g.*, of the phase transformation temperature (T_p) and the metastability of HTPT, are strongly dependent on the measurement conditions [3]. Lee raised questions about whether the polymorphic phase transition actually exists and suggested that the term "HTPT" should be replaced by "*onset of partial polymerization at reaction sites at the surface of solids*" [3]. While some researchers support this viewpoint [4–8], others maintain that they are structural phase transitions [9–12]. Therefore, the high-temperature superprotonic phase behavior remains a controversial subject with an unclear microscopic nature, even though electrical conductivity has been demonstrated to be predominantly protonic [3–12].

In contrast to tetragonal KH_2PO_4, RbH_2PO_4, and $NH_4H_2PO_4$ (space group $I\bar{4}2d$–D_{2d}^{12}) [1–3], monoclinic CsH_2PO_4 (space group $P2_1/m$–C_{2h}^2) [3,13–16], and monoclinic TlH_2PO_4 (space group $P2_1/a$–C_{2h}^5) [17–19] crystals, relatively little work has been done on the low- and high-temperature behaviors of lithium dihydrogen phosphate (LiH_2PO_4). Although the dielectric constant of LiH_2PO_4 has been measured between 300 and 80 K, no discontinuous changes corresponding to a phase transition were observed [20]. LiH_2PO_4 crystallizes in the orthorhombic system with space group $Pna2_1$–C_{2v}^9 with $a = 6.253$, $b = 7.656$, $c = 6.881$ Å, $Z = 4$ (Fig. 1), and a factor group of $mm2$–C_{2v} [21,22]; a point group that can show piezoelectricity and pyroelectricity, and both weak piezoelectric and pyroelectric effects have been observed [21,23]. As shown in Fig. 2, two types of hydrogen bonds have been reported. In the figure, one hydrogen atom, H_1, is in an asymmetric position along the [100] axis [linked by the $O(3)\cdots O(4,4)^{III}$] and the other hydrogen atom, H_2, is in a general position and is involved in an asymmetric bond along the [001] axis [linked by the $O(4)\cdots O(2,2)^{I}$]. These connect the PO_4 tetrahedra,

* Corresponding author. Tel.: +82 553203207; fax: +82 553341577.
E-mail addresses: kwangsei28@hanmail.net, kslee@physics.inje.ac.kr (K.-S. Lee).

0038-1098/$ - see front matter
doi:10.1016/j.ssc.2007.12.011

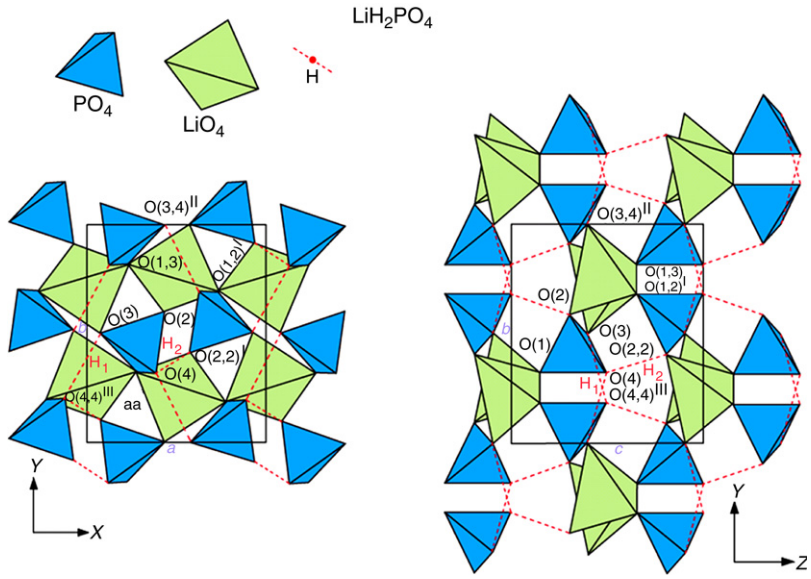

Fig. 1. Projections of the structure of LiH_2PO_4 onto the (001) and (100) planes. Only the oxygen atoms are shown. Dashed lines represent hydrogen bonds (after Catti and Ivaldi, Ref. [22]).

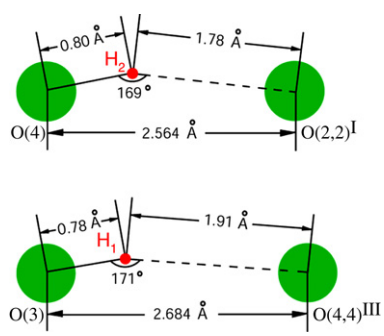

Fig. 2. Two types of hydrogen bonds at room temperature in LiH_2PO_4: $O(3)–H_1 \cdots O(4, 4)^{III}$ along the [100] axis and $O(4)–H_2 \cdots O(2, 2)^{I}$ along the [001] axis (after Catti and Ivaldi, Ref. [22]).

building up a three-dimensional framework. In addition, LiO_4 coordination tetrahedra are linked by vertices and form [100] isolated chains.

In a preliminary study examining both dielectric constants and Raman spectra of LiH_2PO_4 in the 15–1400 cm^{-1} frequency range, Lee et al. found no evidence of a dielectric anomaly from room temperature down to 17 K [24]. Here, we report our reinvestigation of the dielectric constant measurement between 297 and 17 K looking for a possible low-temperature phase transition. We also extended the Raman scattering study at 297, 200, and 70 K between 15–4000 cm^{-1} to obtain a more confident assignment of the external vibrations; spectroscopic evidence for the vibrational modes of LiO_4 in addition to the PO_4 internal vibrations; and O–H vibrations.

2. Experiments

LiH_2PO_4 was synthesized by the reaction $Li_2CO_3 + 2H_3PO_4 \rightarrow 2LiH_2PO_4 + H_2O + CO_2$, and then small, good optical quality single crystals were grown by slow evaporation from the aqueous solution at about 310 K. These crystals were ground to form a disk-shaped pellet to which electrodes could be attached and to perform Raman scattering studies. The powder pellet dielectric constant was measured between 297 and 17 K using an impedance analyzer (HP 4192A). Raman excitation was induced using an argon-ion laser 5145 Å line focused through a cylindrical lens to avoid local heating of the sample. The 45°-scattered light at the polycrystalline surface was dispersed by a double-grating monochromator (Spex 1403) connected to a GaAs photomultiplier tube (Hamamatsu R943-02). The spectral resolution was 2 cm^{-1}. The experimental details were the same as in Ref. [24].

3. Results and discussion

The dielectric constant of the LiH_2PO_4 pellet was measured from 297 to 17 K with cooling at a rate of 0.2 K min^{-1}. As shown in Fig. 3, at 87 kHz and 297 K the dielectric constant was 5.94. Haussühl reported the LiH_2PO_4 single crystal dielectric constant at 293 K between 10 and 100 kHz along the three crystallographic axes as $\varepsilon_{11} = 6.02$, $\varepsilon_{22} = 4.63$, and $\varepsilon_{33} = 7.26$ [23]. For a powder pellet composed of randomly oriented polycrystals, the dielectric constant is averaged as $\varepsilon = \frac{1}{3}(\varepsilon_{11} + \varepsilon_{22} + \varepsilon_{33}) = 5.97$, in good agreement with our measured value of 5.94. As shown in Fig. 3, there was no dielectric anomaly in the given temperature range, indicating that the room-temperature orthorhombic phase persists up to 17 K. However, measurement of the dielectric constant upon heating above room temperature revealed the onset of a thermal transformation near 451 K. Therefore, the behavior of LiH_2PO_4 at high temperatures supplies new information about high-temperature transformation and protonic conductivity in MX_2RO_4-type crystals, which have been reported in a separate paper [25].

The Raman spectral density, $I(\omega)$, is proportional to the imaginary part of the generalized susceptibility, $\chi''(\omega)$: $I(\omega) \propto [n(\omega) + 1]\chi''(\omega)$ where the Bose–Einstein thermal factor, $n(\omega) = (e^{\frac{\hbar\omega}{k_B T}} - 1)^{-1}$ ($\hbar\omega$ is the excitation quanta

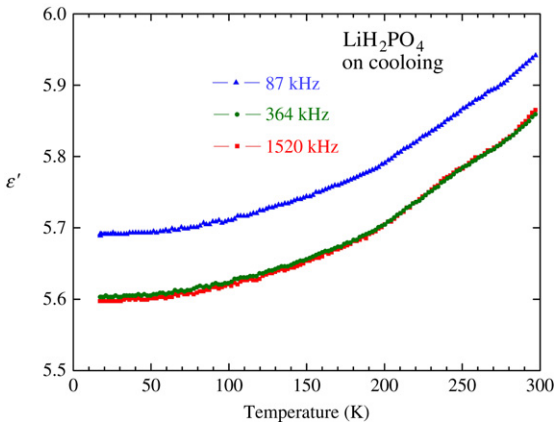

Fig. 3. Temperature dependence of the polycrystalline LiH_2PO_4 dielectric constant.

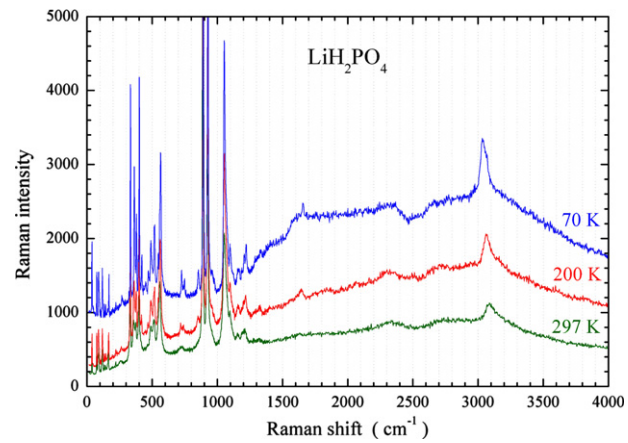

Fig. 4. Polycrystalline LiH_2PO_4 Raman spectra at different temperatures in the 15–4000 cm^{-1} frequency range.

in the sample, k_B, Boltzmann constant, and T, the sample temperature). Fig. 4 shows the LiH_2PO_4 Raman spectra in the frequency range of 15–4000 cm^{-1} at 297, 200, and 70 K. The Raman signals ride on the fluorescent background, and produce very different spectra than tetragonal KH_2PO_4, RbH_2PO_4, and $NH_4H_2PO_4$ (space group $I\bar{4}2d$–D_{2d}^{12}) [1,2,9], monoclinic CsH_2PO_4 (space group $P2_1/m$–C_{2h}^2) [13–15], and monoclinic TlH_2PO_4 (space group $P2_1/a$–C_{2h}^5) [9,17–19]. Even if the crystal structures and symmetries of KH_2PO_4, CsH_2PO_4, and TlH_2PO_4 are different, their crystallographic structures are essentially composed of M^+ (M = K, Cs, Tl) cations and $H_2PO_4^-$ anions. Raman spectra of KH_2PO_4, CsH_2PO_4, and TlH_2PO_4 show almost the same features in the 300–1200 cm^{-1} frequency range [1,2,9,13–15,17–19]. Therefore, these vibrational modes have been assigned as the internal vibrations of a PO_4^{3-} ion modified slightly by the surrounding crystalline field. Very different spectra have been observed in the low-frequency range of 0–300 cm^{-1}, which are related to the lattice vibrations originating from the relative motions between M^+ cations and $H_2PO_4^-$ anions. The vibrational modes of LiH_2PO_4 at 297 K were tentatively assigned according to this scheme in our previous paper [24]. Raman-active vibrational modes were assumed to consist of low- (0–300 cm^{-1}) and high-frequency (300–4000 cm^{-1}) modes. However, this criterion seems problematic, as the crystal structure of LiH_2PO_4 is not composed of Li^+ cations and $H_2PO_4^-$ anions, but of LiO_4 and $H_2PO_4^-$, which share oxygen atoms. Upon cooling a crystal, most lines become narrower with increasing intensity due to the temperature-dependent Bose–Einstein thermal factor $n(\omega)$, as shown in Fig. 4. As some spectral lines, or bands, shift or split in the low-temperature spectra, modes can be assigned with more confidence in the same phase in the 70 K spectra than in the 297 K spectra.

The crystallographic unit cell ($Pna2_1$–C_{2v}^9), which is also a primitive cell, contains four formula units ($Z = 4$) [21,22]. LiH_2PO_4 has eight atoms and therefore $8 \times 4 = 32$ atoms in its primitive cell. The degrees of freedom are derived from the 3 translational and 3 rotational motions. Three of these degrees of freedom are responsible for the acoustic modes of the crystal, leaving $3 \times 32 - 3 = 93$ as the maximum number of optical modes. Four irreducible representations, $A_1(z)$, A_2, $B_1(x)$, and $B_2(y)$, are allowed in its corresponding factor group, $mm2$–C_{2v} [26]. The symmetry species $A_1(z)$, A_2, $B_1(x)$, and $B_2(y)$ are all Raman-active, while those of species $A_1(z)$, $B_1(x)$, and $B_2(y)$ are only active in the infrared spectra.

These spectra may be interpreted by roughly dividing them into four parts on the basis of whether a given mode is associated with collective protonic motions or relaxational motions of the PO_4 and/or LiO_4, external lattice vibrations between PO_4 and LiO_4 (including translations and rotations), internal modes of PO_4 and LiO_4, or vibrations of the hydrogen bonds (stretching and bending). In general, these may be expected to occur in the order of increasing frequency. As the spectral range above 15 cm^{-1} does not cover the collective protonic or relaxational motions of PO_4 and/or LiO_4, we discuss the remaining three regions: external (lattice) vibrations between PO_4 and LiO_4 (including translations and rotations), internal modes of PO_4 and LiO_4, and vibrations of the hydrogen bonds.

3.1. External vibrations

Consider the group of n nonequivalent points contained in the primitive unit cell. Subtracting the three pure translations (acoustic vibrations) leaves one with $3n - 3$ optical modes. The object is to classify these vibrations as external or internal, where the LiH_2PO_4 internal vibrations arise from PO_4 and LiO_4 motion, and the external vibrations, commonly known as lattice vibrations, result from the relative motion between the groups. The optical phonons are divided into translational and rotational (or librational) types, which, in the limit of vanishing forces among the groups, correspond to pure translations and pure rotations. As mentioned above, the LiO_4 tetrahedron shares oxygen atoms with its four neighboring PO_4 tetrahedra, so that the decoupling of the motions of PO_4 and LiO_4 is not as simple as in MH_2PO_4, which is composed of M^+ and $H_2PO_4^-$. In addition, the hindered rotational modes of PO_4 and LiO_4 can be excited. The low-frequency (15–300 cm^{-1}) region in Fig. 5 is assigned to external modes with a naive

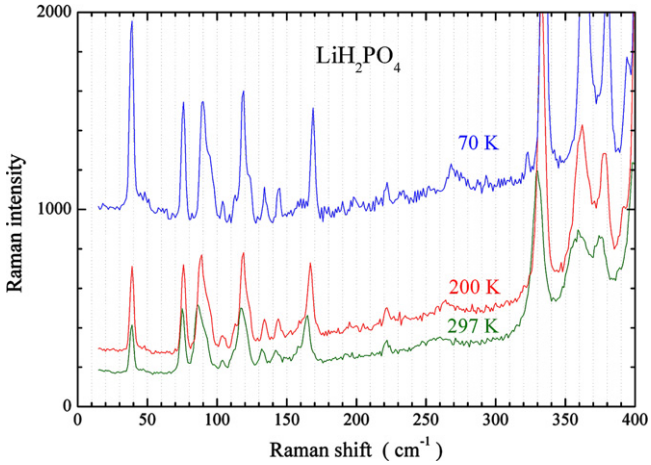

Fig. 5. Low-frequency Raman spectra of polycrystalline LiH_2PO_4 at different temperatures in the 15–400 cm^{-1} range, showing mainly the external vibrations as well as part of the internal vibrations of PO_4 and LiO_4.

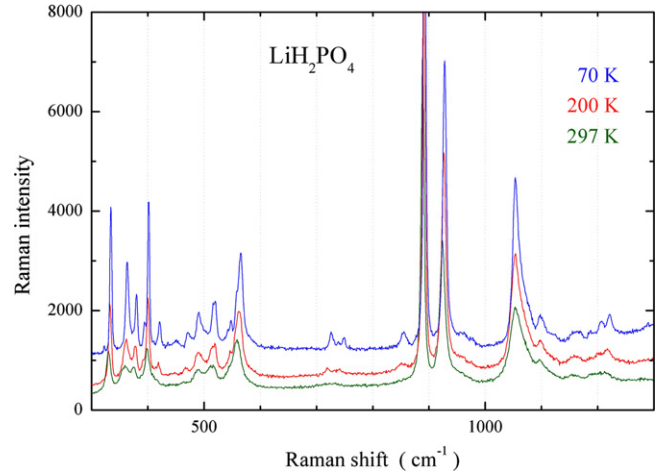

Fig. 6. High-frequency Raman spectra of polycrystalline LiH_2PO_4 at different temperatures in the 300–1300 cm^{-1} range, showing the internal vibrations of PO_4 and LiO_4 and some parts of the in-plane δ (O–H) and out-of-plane γ (O–H) bending modes of hydrogen vibrations.

interpretation given in Table 1. As shown in Fig. 5, at 70 K in the frequency range of 200–300 cm^{-1}, the intensity of the weak shoulders, or bands, increases with decreasing temperature. Consequently, distinguishing between external and internal modes is not intuitively obvious. Recently, Shchur calculated the lattice dynamics of CsH_2PO_4 [16]; a similar lattice-dynamical calculation should be helpful in analyzing the Raman spectra of LiH_2PO_4.

3.2. *Internal vibrations of* PO_4 *and* LiO_4

The free tetrahedral phosphate anion PO_4, with $\bar{4}3m$–T_d symmetry, has nine vibrational normal modes, all of which are Raman-active: the non-degenerate and completely symmetrical A_1 mode (stretching mode ν_1), the doubly degenerate E modes (bending modes ν_2), and two triply degenerate F_2 modes (stretching modes ν_3 and bending modes ν_4). The values for the frequencies of these modes in the solution reported in the literature are $\nu_1 \approx 980$ cm^{-1}, $\nu_2 \approx 363$ cm^{-1}, $\nu_3 \approx 1082$ cm^{-1}, and $\nu_4 \approx 515$ cm^{-1} [27]. Examining the non-cubic local site symmetry of the PO_4^{3-} ion in the crystal lattice, the molecular vibrations of the PO_4^{3-}ion are modified slightly by the surrounding crystalline field. The lines, shoulders, and bands of the internal vibrations of the PO_4^{3-}ion in Fig. 6 will be assigned by referring to the frequencies of the PO_4^{3-}modes in the solution (Table 1). In addition to the PO_4 tetrahedron, LiH_2PO_4 also has a LiO_4 tetrahedron [21,22]. This is a peculiar structural aspect of LiH_2PO_4 compared to other MX_2RO_4-type crystals (M = K, Rb, NH_4, Cs, Tl; X = H, D; R = P, As) without MO_4 tetrahedra. Therefore, the LiO_4 internal modes are able to excite LiH_2PO_4. The oxo-anions form a very large group, and the central atom may be a member of any group in the periodic table. The only species containing a group I element is the LiO_4 tetrahedron, which exists in Li_2CO_3, the spinel $LiFeCr_4O_8$, Li_2MoO_4, and Li_2WO_4 all of which have the phenacite (Be_2SiO_4) structure. Bands assigned to the LiO_4 tetrahedron on the basis of ^{7}Li–^{6}Li shifts occur at 497, 435, 416, 397 cm^{-1} (Li_2CO_3); 461 cm^{-1} (spinel); 471, 452 cm^{-1} (Li_2WO_4); and 464, 432, 391 cm^{-1} (Li_2MoO_4) [28]. Similarly, the lines or shoulders in the 390–500 cm^{-1} frequency range of LiH_2PO_4 of Fig. 6 may be assigned as the internal modes of LiO_4. This frequency range overlaps with those of ν_2 (PO_4) and ν_4 (PO_4), and may complicate the assignment of internal modes of LiH_2PO_4. As the LiO_4 tetrahedron shares oxygen atoms with its four PO_4 tetrahedra neighbors (Fig. 1), the decoupling between the motions of the two tetrahedra is not clear-cut. Using the relationship between crystallographic point groups and their subgroups [29], the site symmetry of PO_4 of LiH_2PO_4 is anticipated to be $1 - C_1$ as is the site symmetry of the LiO_4 of LiH_2PO_4. In contrast, local site symmetries for PO_4 in KH_2PO_4, CsH_2PO_4, and TlH_2PO_4 have been reported as $\bar{4} - S_4$ [1,2,9], $m - C_s$ [13–15], and $1 - C_1$ [9,17–19], respectively. In addition to the fundamentals of PO_4 and LiO_4, overtones and combinations of PO_4 and LiO_4 can appear in the Raman spectra, and it is therefore necessary to take overtones and combinations into consideration for definite mode assignments (Table 1). To definitely identify the LiO_4 tetrahedron modes, the ^{7}Li–^{6}Li isotopic shift should be measured.

3.3. *O–H vibration*

Due to a certain anharmonicity of the hydrogen bond, the hydrogen vibrations are expected to be very complex. As the low-frequency modes, or bands, are often referred to as collective proton modes, and the high-frequency complex broad bands above 1500 cm^{-1}, as O–H stretching vibrations, the hydrogen modes are expected to be exhibited through the whole Raman spectra range (0–4000 cm^{-1}). According to Novak, O–H···O hydrogen bonding in solids is classified as strong, intermediate, or weak [30]. There is an empirical correlation between the stretching ν (O–H) frequency and the R(O···O) distances of 2.40–2.60 Å, 2.60–2.70 Å, and >2.70 Å, for the strong, intermediate, and weak bonds, respectively. As the distance becomes longer, the bond weakens and the ν (O–H) frequency increases to 700–2700 cm^{-1} for the strong,

Table 1
Raman frequencies (cm^{-1}) tentatively assigned to external and internal vibrations of polycrystalline LiH_2PO_4 at 70 K

Frequency (cm^{-1})	Possible assignments	Frequency (cm^{-1})	Possible assignments
39 m		451 w	ν_4 (PO_4) or LiO_4
48 w		471 m	ν_4 (PO_4) or LiO_4
61 w		491 m	ν_4 (PO_4) or LiO_4
68 w		496 sh	ν_4 (PO_4) or LiO_4
76 m		516 s	ν_4 (PO_4)
82 w		520 s	ν_4 (PO_4)
90 m		543 w	ν_4 (PO_4)
94 sh		548 m	ν_4 (PO_4)
104 w		558 s, sh	ν_4 (PO_4)
109 w			
113 w			
119 m		565 s	ν_4 (PO_4)
123 sh		726 m	overtone of PO_4 or LiO_4
129 w	Lattice vibrations	739 m	overtone of PO_4 or LiO_4
134 w		749 m	overtone of PO_4 or LiO_4
141 w		855 m	overtone of PO_4 or LiO_4
145 w			
153 w			
160 w		892 vs	ν_1 (PO_4)
169 m		928 s	ν_1 (PO_4)
178 w		958 w, sh	γ (O–H)
190 w		975 w, sh	γ (O–H)
198 w			
222 w			
233 w		1053 s	ν_3 (PO_4) or γ (O–H)
250 w		1070 s, sh	ν_3 (PO_4) or γ (O–H)
268 w		1098 m	ν_3 (PO_4) or γ (O–H)
278 w		1120 w	ν_3 (PO_4) or γ (O–H)
287 w		1163 w	ν_3 (PO_4) or γ (O–H)
293 w		1187 w	ν_3 (PO_4) or γ (O–H)
		1207 m	ν_3 (PO_4) or γ (O–H)
309 w	ν_2 (PO_4)	1222 m	ν_3 (PO_4) or γ (O–H)
323 w	ν_2 (PO_4)		
334 s	ν_2 (PO_4)	1282 w	δ (O–H)
363 s	ν_2 (PO_4)	1327 w	δ (O–H)
380 s	ν_2 (PO_4)	1469 sh, b	
394 m	ν_2 (PO_4) or LiO_4	1655 m	$C\nu$ (O–H_2)
402 s	ν_2 (PO_4) or LiO_4	1844 w, b	
411 w	ν_2 (PO_4) or LiO_4	2069 w, b	
421 m	ν_2 (PO_4) or LiO_4	2312 w, b	$B\nu$ (O–H_2)
436 w	ν_2 (PO_4) or LiO_4	2770 w, b	$A\nu$ (O–H_2)
		3032 s	ν (O–H_1)
		3080 s, sh	ν (O–H_1)

Intensity: - s: strong ; m: medium; w: weak ; v: very ; b: broad ; sh: shoulder.

2800–3100 cm^{-1} for the intermediate, and >3200 cm^{-1} for the weak. According to this scheme, two types of LiH_2PO_4 hydrogen bonds can be described together, with the first, an intermediate type, having a hydrogen atom, H_1, in an asymmetric position along the [100] axis [$R(O_3–H\cdots O_4)$ = 2.684 Å] and the second, belonging to strong type having the hydrogen atom, H_2, in a general position and involved in an asymmetric bond along the [001] axis [$R(O_4–H_2\cdots O_2)$ = 2.564 Å]. The relatively sharp band near 3085 cm^{-1} at 297 K in Fig. 7 is designated as a vibration of O–H_1 belonging to an intermediate hydrogen bond, while the three broad bands near 2758, 2314, 1630 cm^{-1} at 297 K are designated as the *A*, *B*, *C* bands of O–H_2 and belong to strong hydrogen bonds

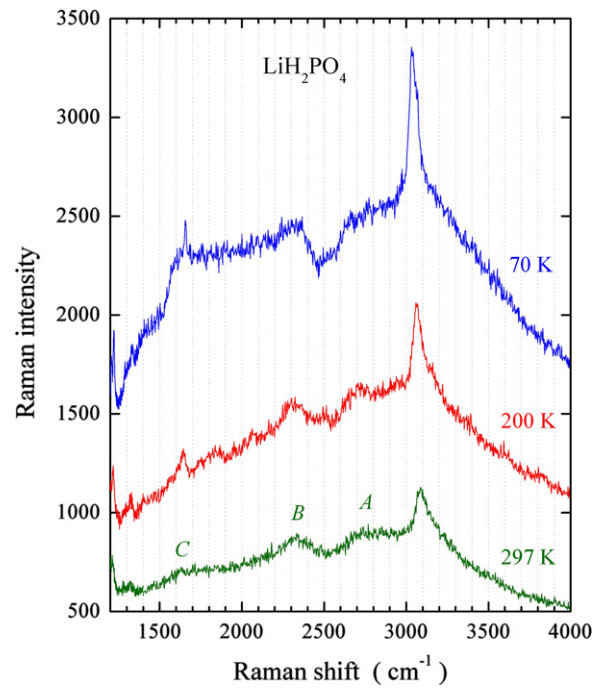

Fig. 7. High-frequency Raman spectra of polycrystalline LiH_2PO_4 at different temperatures in the 1200–4000 cm^{-1} range, showing principally the internal vibrations of O–H.

(Table 1). The absence of ferroelectricity in LiH_2PO_4 seems due to the structural asymmetry of hydrogen bonds. Although the LiH_2PO_4 does not undergo a ferroelectric phase transition, the general three bands (*A*, *B*, *C* bands) characteristics persist but with complex splitting upon cooling, as shown in Fig. 7. The interpretation of this spectral range should include the in-plane δ (O–H) and out-of-plane γ (O–H) bending modes of hydrogen vibrations as well as the stretching ν (O–H_1) mode. The in-plane deformation vibrations δ (O–H_1) and δ (O–H_2) give rise to bands in the 1200–1300 cm^{-1} region, while the out-of-plane γ (O–H_1) and γ (O–H_2) modes appear in the 900–1100 cm^{-1} region [30].

4. Conclusions

Measurements of the dielectric constant of LiH_2PO_4 presented no evidence of a phase transition between 297 and 17 K. The low-frequency (15–300 cm^{-1}) region in Raman spectra was naively assigned to external modes. In the frequency range from 200–300 cm^{-1}, lowering the temperature from 297 to 70 K increased the intensities of the weak shoulders, or bands, precluding clear determination of external versus internal modes. The vibrational modes appearing over the 390–500 cm^{-1} range were assigned as the internal modes of the LiO_4 tetrahedra. This frequency range overlapped those of ν_2 (PO_4) and ν_4 (PO_4). The O–H vibration frequencies of LiH_2PO_4 were in good agreement with the findings of crystallographic reports that there are two types of hydrogen bonds: an intermediate (long bond) and a strong (short bond). To obtain accurate measurements of the vibrational frequencies of the symmetry species, and reasonable assignment of the vibrational modes, spectroscopic studies of single crystals and

^{7}Li–^{6}Li isotopic substitution should be made and a group-theoretical analysis of the vibrational modes undertaken.

Acknowledgments

This work was supported by the 2005 Inje University research grant and partially by the Korea Research Foundation Grant funded by the Korean Government (MOEHRD, Basic Research Promotion Fund) (KRF-2006-331-C00088).

References

[1] See, *e.g.*, KH_2PO_4-type Ferro- and Antiferroelectrics, Ferroelectrics 71 (1987) (special issues).
[2] See, *e.g.*, KH_2PO_4-type Ferro- and Antiferroelectrics, Ferroelectrics 72 (1987) (special issues).
[3] K.-S. Lee, J. Phys. Chem. Solids 57 (1996) 333.
[4] E. Miller, T. Land, P. Whitman, UCRL-ID-142259, Lawrence Livermore National Laboratory, Livermore, CA, 2001.
[5] J.-H. Park, K.-S. Lee, B.-C. Choi, J. Phys. Condens. Matter 13 (2001) 9411.
[6] K.-S. Lee, Ferroelectrics 268 (2002) 369.
[7] J.E. Diosa, R.A. Vargas, I. Albinsson, B.-E. Mellander, Phys. Status Solidi (b) 241 (2004) 1369.
[8] R.H. Chen, C.-C. Yen, C.S. Shern, T. Fukami, Solid State Ion. 177 (2006) 2857.
[9] J.A. Subramony, B.J. Marquardt, J.W. Macklin, B. Kahr, Chem. Mater. 11 (1999) 1312.
[10] D.A. Boysen, S.M. Haile, H. Liu, R.A. Secco, Chem. Mater. 15 (2003) 727.
[11] S.M. Haile, C.R.I. Chisholm, K. Sasaki, D.A. Boysen, T. Uda, Faraday Discuss. 134 (2007) 17.
[12] Y.-K. Taninouchi, T. Uda, Y. Awakura, A. Ikeda, S.M. Haile, J. Mater. Chem. 17 (2007) 3182.
[13] B. Marchon, A. Novak, J. Chem. Phys. 78 (1983) 2105.
[14] S. Rumble, F. Ninio, S.S. Ti, Solid State Commun. 42 (1982) 767.
[15] F. Romain, A. Novak, J. Mol. Struct. 263 (1991) 69.
[16] Y. Shchur, Phys. Rev. B 74 (2006) 054301.
[17] P.V. Huong, M. Couzi, J.R. Vignalou, A. Tranquard, in: M. Balkanski, R.C.C. Leite, S.P.S. Porto (Eds.), Proceedings of the Third, International Conference on Light Scattering in Solids, Campinas, Brazil, Wiley, New York, 1975, p. 845.
[18] B. Pasquier, N. Le Calve, S.A. Homsi-Teiar, F. Fillaux, Chem. Phys. 171 (1993) 203.
[19] K.-S. Lee, D.-H. Ha, Phys. Rev. B 48 (1993) 73.
[20] J. Le Bot, S. Le Montagner, Y. Allain, C. R. Acad. Sci. 236 (1953) 1409.
[21] F. Remy, B. Bachet, Bull. Soc. Chim. France (1967) 1699.
[22] M. Catti, G. Ivaldi, Z. Kristallogr. 146 (1977) 215.
[23] S. Haussühl, Cryst. Res. Technol. 31 (1996) 323.
[24] K.-S. Lee, J.-H. Ko, V.H. Schmidt, J. Korean Phys. Soc. 46 (2005) 104.
[25] K.-S. Lee, J. Moon, J. Lee, M. Jeon, Solid State Commun. (in press).
[26] G. Turrell, Infrared and Raman Spectra of Crystals, Academic Press, London, 1972, p. 331.
[27] G. Herzberg, Molecular Spectra and Molecular Structure II. Infrared and Raman Spectra of Polyatomic Molecules, Van Nostrand, Toronto, 1945, p. 167.
[28] S.D. Ross, Inorganic Infrared and Raman Spectra, McGraw-Hill, London, 1972, p. 117, 202 and 216.
[29] G. Turrell, Infrared and Raman Spectra of Crystals, Academic Press, London, 1972, p. 338.
[30] A. Novak, Structure and Bonding, vol. 18, Springer-Verlag, 1974, p. 177.